Journal of Neural Engineering

PAPER

Chronic intracochlear electrical stimulation at high charge densities: reducing platinum dissolution

Robert K Shepherd[1,2,5] , Paul M Carter[3] , Ya Lang Enke[3] , Alex Thompson[1,2] , Brianna Flynn[1], Ella P Trang[1] , Ashley N Dalrymple[1,4] and James B Fallon[1,2]

[1] Bionics Institute, St Vincent's Hospital, Melbourne, Australia
[2] Medical Bionics Department, The University of Melbourne, Melbourne, Australia
[3] Cochlear Ltd, Sydney, Australia
[4] Department of Physical Medicine and Rehabilitation, University of Pittsburgh, Pittsburgh, PA, United States of America

E-mail: rshepherd@bionicsinstitute.org

Abstract

Objective. Cochleae of long-term cochlear implant users have shown evidence of particulate platinum (Pt) corroded from the surface of Pt electrodes. The pathophysiological effect of Pt within the cochlea has not been extensively investigated. We previously evaluated the effects of Pt corrosion at high charge densities and reported negligible pathophysiological impact. The present study extends this work by examining techniques that may reduce Pt corrosion.
Approach. Deafened guinea pigs were continuously stimulated for 28 d using biphasic current pulses at extreme charge densities using: (i) electrode shorting; (ii) electrode shorting with capacitive coupling (CC); or (iii) electrode shorting with alternating leading phase (AP). On completion of stimulation, cochleae were examined for corrosion product, tissue response, auditory nerve (AN) survival and trace levels of Pt; and electrodes examined for surface corrosion.
Main results. Pt corrosion was evident at ≥ 200 μC cm^{-2} phase^{-1}; the amount dependent on charge density ($p < 0.01$) and charge recovery technique ($p < 0.01$); reduced corrosion was apparent using CC. Tissue response increased with charge density ($p < 0.007$); cochleae stimulated at ≥ 200 μC cm^{-2} phase^{-1} exhibited a vigorous response including a focal region of necrosis and macrophages. Notably, tissue response was not dependent on the charge recovery technique ($p = 0.56$). Despite stimulation at high charge densities resulting in significant levels of Pt corrosion, there was no stimulus induced loss of ANs. *Significance.* Significant increases in tissue response and Pt corrosion were observed following stimulation at high charge densities. Charge recovery using CC, and to a lesser extent AP, reduced the amount of Pt corrosion but not the tissue response. Stimulation at change densities an order of magnitude higher than those used when programming cochlear implant recipients in the clinic, produced a vigorous tissue response and corrosion products without evidence of neural loss.

1. Introduction

Platinum (Pt) is the most common electrode material used in commercial neural prostheses [1]. It has a long clinical history as a safe and effective electrode material when used in conjunction with stimulation via reversible Faradaic reactions [2, 3]. Nevertheless, clinical studies examining cochleae from cochlear implant users have shown Pt deposits in the

tissue capsule surrounding the electrode array [4–7]. Some of these reports also described an increased tissue reaction associated with the Pt [6, 7].

We recently demonstrated in an animal model of cochlear implantation, that four weeks of continuous stimulation using high charge densities (267 & 400 μC cm^{-2} phase^{-1}); approximately an order of magnitude greater than typical clinical levels (median bipolar: 50 μC cm^{-2} phase^{-1}; monopolar: ~10 μC cm^{-2} phase^{-1}), resulted in significant amounts of Pt within the tissue capsule proximal to the electrode array [8]. Notably, the

---

[5] Author to whom any correspondence should be addressed.

generation of this corrosion product was not associated with an increased loss of primary auditory neurons (ANs). Moreover, cochleae stimulated at 267 or 400 μC cm^{-2} phase^{-1} exhibited a widespread tissue reaction including evidence of necrosis close to the electrode. In contrast, cochleae stimulated at 100 μC cm^{-2} phase^{-1} showed no clear evidence of Pt corrosion and only a minimal tissue response.

Safe electrical stimulation of neural tissue is achieved by the creation of a capacitive layer at the electrode–tissue interface known as the Helmholtz double layer, and a series of electrochemical reactions that convert the charge carriers from electrons (in the electrode) to ions (in the electrolyte) [3, 9, 10]. At low charge densities (<20 μC cm^{-2} phase^{-1}), the charge injection process is dominated by capacitive mechanisms; no electrochemical reaction products are formed within the electrolyte [11, 12]. With increasing charge density, reversible electrochemical Faradaic reactions begin to take over the charge injection process [3, 9]. These reactions are localized to the electrode surface and can be reversed via the passage of an equal charge of opposite polarity, ensuring that no new electrochemical species are released into the biological environment [9, 11, 12]. At higher charge densities, charge injection is increasingly achieved via a number of irreversible electrochemical reactions, resulting in the release of electrode corrosion products, electrolysis of water, and oxidation of chloride ions [11]. These electrochemical reaction products diffuse from the electrode and cannot be reversed, resulting in direct current (DC) [13]. Local pH changes [14, 15], the formation of reactive oxygen species, and tissue damage [16], can also occur. Protection against charge imbalance is usually achieved in clinical settings by shorting electrodes between current pulses, stimulating using charge densities well within the water window, and/or the use of electrode shorting with coupling capacitors (CCs) [17].

We have previously shown that electrode shorting with CC [13] and electrode shorting with alternating leading phase (AP) [14] can reduce residual DC levels *in vivo*. In the present study we compared the use of electrode shorting alone, with electrode shorting and CC, and electrode shorting and AP, in a series of chronic stimulation studies using a wide range of charge densities (0, 100, 200, 228, 267, 400 or 540 μC cm^{-2} phase^{-1}) and stimulus rates (200 or 1000 pulses per second (pps)). We show that the level of Pt corrosion within stimulated cochleae is highly dependent on charge density, while the use of electrode shorting with CC, and to a lesser extent electrode shorting with AP, appears to reduce Pt corrosion. Tissue response within the implanted cochlea is also significantly dependent on charge density; however, it is *not* related to the extent of Pt corrosion product within the cochlea. Finally, although stimulated at charge densities which are an order of magnitude higher than those used when programming cochlear implant recipients in the clinic, evoking a vigorous tissue response and Pt deposits, there was no stimulus induced neural loss. The present findings have implications for both cochlear implants and other neural prostheses that use Pt electrodes.

2. Methods

The majority of the methods used have been presented in detail in [8] and are therefore only briefly described here.

2.1. Experimental subjects
Twenty-four guinea pigs were used in this study. Additional data from the 19 animals described in our previous study [8] were included in the present analysis resulting in a total of 43 animals. These animals are identified in table 1. All procedures were approved by the Bionics Institute Animal Research Ethics Committee and followed the principles of the US National Institutes of Health guidelines for the care and use of animals for research.

2.2. Auditory brainstem responses
Normal hearing status was established using click-evoked auditory brainstem responses (ABRs; threshold <50 decibels peak equivalent sound pressure level [dB p.e. SPL] re 20 μPa). Under general anaesthesia, ABRs were recorded using subcutaneous (s.c.) electrodes (vertex positive; neck negative; thorax ground) with the animal anesthetised (1%–2% isoflurane in oxygen, 1 l min^{-1}; Isoflo; Zoetis, UK).

2.3. Deafening protocol
Under general anaesthesia each animal was deafened by co-administration of frusemide (130 mg kg^{-1}; Ilium, Australia) and kanamycin sulfate (420 mg kg^{-1}, s.c.; Sigma-Aldrich, USA) [18]. Seven days following deafening hearing status was retested; only animals that exhibited a $\geq$50 dB increase in threshold were included in the study.

2.4. Scala tympani electrode array
HL electrode arrays containing eight smooth Pt electrodes were used in this study (Cochlear Ltd., Australia; figure 1). During stimulation charge per phase was held constant (0.2 μC phase^{-1}) allowing charge density to be controlled by varying the geometric surface area of the Pt contacts on the array. Each electrode array had Pt contact areas of either: 0.2, 0.1, 0.0875, 0.075, 0.05 or 0.0375 mm^2 achieved by laser ablation of the polydimethylsiloxane (PDMS) overlaying each electrode. The charge density associated with these electrode arrays were 100, 200, 228, 267, 400 or 540 μC cm^{-2} phase^{-1} respectively.

2.5. Cochlear implant surgery
Two weeks after deafening each animal was anaesthetized (isoflurane; 2%–2.5% in oxygen [1 l min^{-1}]), the
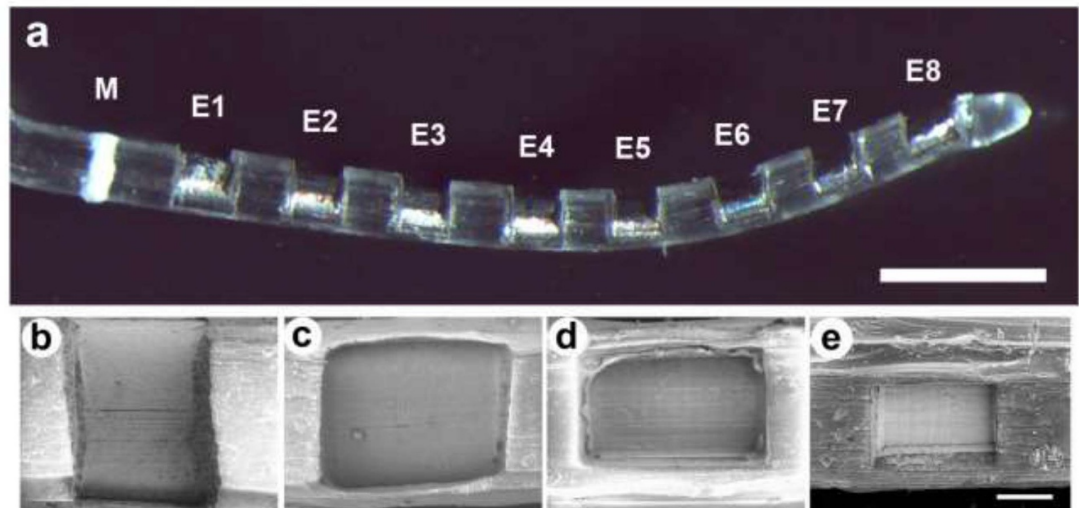
Figure 1. (a) A HL8 electrode array illustrating the 8 Pt electrodes (E1–E8) on a PDMS silicone carrier. Electrode 1 (E1) was the most basal and electrode 8 (E8) the most apical electrode. All electrode surface areas on each array were identical. Scale bar = 1 mm. (b)–(e) Scanning electron micrographs showing four of the electrode contacts used in the study; (b) 0.2 mm^2; (c) 0.085 mm^2; (d) 0.075 mm^2; and (e) 0.0375 mm^2. Scale bar = 100 μm.

left cochlea was surgically exposed, the round window incised, and the electrode array inserted as far as the upper basal (UB) turn scala tympani [8]. There was no surgery on the right cochlea which functioned as a deafened, unimplanted control.

2.6. Electrode impedance

The voltage transient impedance of each electrode was measured using both common ground and bipolar electrode configurations periodically during the course of chronic stimulation [19]. Impedance was monitored by recording the peak voltage transient during the first phase in response to a 100 μs phase^{-1} biphasic current pulse of 100 μA.

2.7. *Electrically-evoked* ABRs

Electrically-evoked ABRs (EABRs) were recorded immediately following surgery and on completion of the 28 d stimulation program [20]. Biphasic current pulses were used to stimulate adjacent bipolar electrodes along the electrode array. Recordings were made at intensity intervals presented randomly from below threshold to a maximum of 250 Current Level (CL; where current in μA = 17.5 × (100$^{(CL/255)}$)). Two recordings were made at each CL and threshold was defined as the lowest stimulus intensity required to elicit a clear EABR with amplitude of at least 0.2 μV for both responses. Threshold detection was performed with the observer blinded to the treatment history.

2.8. Chronic stimulation program

Immediately following surgery and EABR recordings, each animal was connected to a portable stimulator [21] delivering 100 μs phase^{-1} charge-balanced biphasic current pulses at 200 or 1000 pps at a charge/phase of 0.2 μC phase^{-1} [8]. Animals were continuously stimulated for 28 d using two tripolar electrode configurations with E4 and E7 as the centre tripoles. A cathodic first phase was delivered to the centre electrode while the two flanking electrodes formed the return path. All currents were reversed in the second phase. The centre electrodes generated charge densities of 100, 200, 228, 267, 400 or 540 μC cm^{-2} phase^{-1} (E4 and E7; table 1), spanning a range of charge densities both within and significantly greater than the maximum recommended industry standard of 216 μC cm^{-2} phase^{-1} [22]; while flanker electrodes developed approximately half this charge density (E3, E5; E6 and E8; table 1). Two electrodes on each array (E1 & E2) served as unstimulated controls.

While charge-balanced current pulses significantly reduce the level of potentially damaging DC, stimulators typically use additional techniques in order to minimise any residual DC component. In the present study, charge-balance was achieved using one of three techniques (table 1): (i) stimuli for cohorts 2–5 and 8 were charge-balanced using electrode shorting between current pulses [17], whereby electrodes are shorted together at a time when no current is delivered to ensure that any net charge during the previous stimulation pulse is recovered, a technique that was used exclusively in our previous study [8]; (ii) cohorts 7 & 9 used both electrode shorting and CC, where 1 μF capacitors were placed in series with each electrode between the stimulator current source and the electrode contact; and (iii) cohort 6 used electrode shorting with AP—i.e. the polarity of the leading phase was alternated for each current pulse.

If stimulation using the tripolar configuration was not possible due to high electrode impedance

(>25 kΩ) or lead wire breakage, stimulation of that tripolar electrode ceased.

2.9. Histology

Following 28 d of continuous stimulation each animal was euthanized with sodium pentobarbitone and systemically perfused with 10% neutral buffered formalin. The electrode array was removed for examination under a scanning electron microscope (SEM; see below). Stimulated and contralateral control cochleae were decalcified, frozen, and cryo-sectioned at 12 μm to the mid-modiolar point. The second half of each cochlea was kept for trace analysis of Pt using inductively coupled plasma mass spectrometry (ICP-MS; see below; [8]).

Serial histological sections from each cochlea were stained with haematoxylin and eosin (H&E) for qualitative examination [23]. AN survival, measured as neural density, and tissue response in the scala tympani were determined. ANs were counted in midmodiolar sections. ANs within Rosenthal's canal in the lower basal (LB), UB, lower middle (LM), upper middle (UM) and the apical (A) cochlea were recorded [8, 23]. Rosenthal's canal area was measured using Image J version 1.52p and the density of the ANs was calculated. The AN density for each cochlear region was averaged from 5 sections spaced at least 72 μm apart to ensure that no AN was counted twice.

To quantify the tissue reaction, the extent of fibrosis was measured at six locations along the electrode array (two each in the LB, UB and LM turns). The area of the scala tympani was measured and the 'Triangle' algorithm (Image J) was applied to automatically threshold the tissue response. The area of scala tympani excluding the area of the electrode array was recorded and the percentage of the scala tympani occupied by the tissue was determined.

In addition to quantifying the extent of the tissue response in implanted cochleae, the nature of the inflammatory response adjacent to the electrode array was examined and the extent of any necrotic and/or dense macrophage response was assessed by measuring the thickness of these zones in the section of each cochlea displaying the most extensive response (e.g. figure 2). Histological images were digitized using a Zeiss AxioLab microscope and the zone thickness measured using Image J software.

If present, the necrotic zone was identified by the presence of amorphous material and was surrounded by a band of macrophages [8]. The macrophage zone was usually surrounded by mature fibrous tissue that occupied large regions of the scala tympani.

Each cochlea was also examined for evidence of electrode insertion trauma. All histological sections were examined under a microscope by a researcher experienced in cochlear histopathology. Insertion trauma was identified by fracture of the osseous spiral lamina and/or tears to the basilar membrane or the outer cochlear wall. This form of trauma evokes a
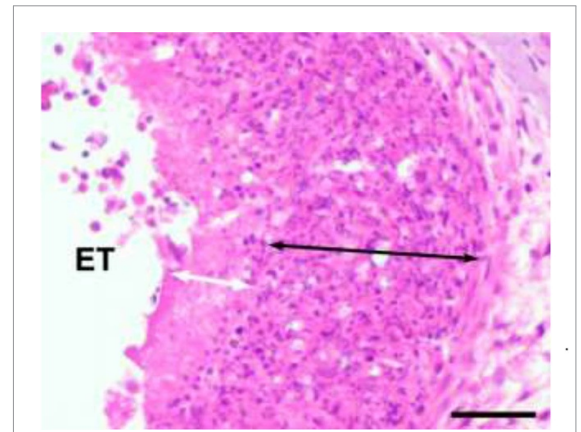

Figure 2. Example illustrating the technique used to measure the width of the necrotic zone containing only cellular debris (white arrow), and the macrophage zone (black arrow). A necrotic zone was only occasionally observed, while a macrophage zone was commonly observed and located between the electrode array and loose fibrous tissue which typically occupied the remainder of the scala tympani. ET = electrode tract. Scale bar = 50 μm.

clear histopathological signature including a vigorous tissue response; neo-osteogenesis; loss of ANs and an increased acute inflammatory response [19, 24].

Finally, each cochlea was also examined histologically for the presence of dense particulate material observed within the tissue capsule [8]. The extent of this material was qualitatively graded from 0–4 (0, no particulate material evident in any section; 1, possible particulate material present; 2, clear localised particulate material present; 3, particulate material present in a number of sections; 4, widespread particulate material present).

2.10. Scanning electron microscopy

Each electrode array was rinsed, ultrasonically cleaned in distilled water, and stored in 70% ethanol until SEM examination. A small number of electrode arrays required additional cleaning in Enzol (diluted 1:40 for 1 h at room temperature; WPI Inc. USA) to remove organic matter and allow examination of the underlying Pt electrode surface. All electrodes were examined using a FEI QUANTA 200 SEM and photographed at low (×600) and medium magnifications (×2000). A region of each electrode surface was then randomly selected and photographed at higher magnifications (×4000 and ×10 000). The surface condition of each Pt electrode was evaluated by an investigator blinded to the experimental groups. Each electrode surface was examined for evidence of mechanical damage, pitting corrosion and surface deposits, and the corrosion graded from 0–5 (0, no corrosion; 1, no evidence of corrosion but electrode partially coated with organic material; 2, localized minor corrosion; 3, localized moderate corrosion; 4, widespread corrosion; 5, severe and extensive corrosion) [8, 25, 26].

Table 1. Summary of the cohorts used in this study.

Cohort	Charge per phase (μC phase^{-1})	Centre electrode[a] charge density (μC cm^{-2} phase^{-1})[b]	Flanker electrode charge density (μC cm^{-2} phase^{-1})	Charge recovery technique	Stimulus rate (pps)	N (cochleae)
1[§]	0	0	0	N/A	N/A	4
2[§]	0.2	100	50	ES	200	5
3	0.2	200	100	ES	1000	4
4	0.2	228	114	ES	200	3
5[§]	0.2	267	133	ES	200	5
6	0.2	267	133	ES & AP	200	5
7	0.2	267	133	ES & CC	200	6
8[§]	0.2	400	200	ES	200	5
9	0.2	540	270	ES & CC	200	6

[a]The cited charge density refers to the centre electrode of the tripole.[b]Geometric surface area. [§]Cohorts reported in [8]. N/A, not applicable; ES, Electrode shorting; AP, alternating leading phase; CC, coupling capacitor in series with stimulator output.

Finally, unstained histological sections were examined under the SEM to identify particulate matter observed in some cochleae. Elemental analysis using an INCA X-Act SDD EDS system with an Oxford Aztec Microanalysis System (3.1) was used to compare cochlear regions containing particulate material with adjacent regions containing only fibrous tissue [8].

2.11. Trace analysis of Pt

The second half of each cochlea was used to measure trace levels of Pt using ICP-MS. This was performed by the National Measurement Institute of the Australian Government using an Agilent 7700X ICP-MS system. Both the implanted and contralateral (control) cochleae were examined for Pt. Because tissue samples were required to be >0.5 g for analysis, cochlear tissue within each cohort was combined into a single analysis sample. Pt trace analysis was reported as the mass of Pt per mass of tissue in each half cochlea [8].

2.12. Statistical analysis

All statistical analysis was performed using SigmaPlot version 13.0 (Systat Software, Inc.). A 2 way repeated measures analysis of variance (RM ANOVA; electrode and time) was used to compare both EABR and electrode impedance data for stimulated versus implanted control cochleae. AN density for stimulated versus contralateral unimplanted cochlea was also compared using RM ANOVA (side and region). Finally, a Kruskal-Wallis 1 way ANOVA (stimulated versus control) with post hoc comparisons made using Dunn's method, was used to compare the tissue response within the scala tympani and the degree of Pt deposits within the cochlea. Data are presented as mean and standard error of the mean (sem). An alpha level <0.05 was used to indicated significance for all tests. All EABR thresholds; histological techniques (including AN survival, tissue response, thickness of both the necrotic and macrophage zones); and SEM analysis of the Pt electrodes were performed using appropriate blinded techniques.

3. Results

3.1. Electrode impedance

Fifteen percent of the electrodes went open circuit as a result of leadwire breakage during the chronic stimulation program. This percentage was slightly higher than the implanted non-stimulated control animals (10% open circuit). Once open circuit, the electrode was withdrawn from further analysis. The functional electrodes showed a small but significant increase in impedance (12.2 ± 0.7 to 14.7 ± 1.2 kΩ) over the duration of the stimulation program ($p = 0.035$; Two way (Electrode, Time) RM ANOVA).

3.2. Electrically-evoked responses

There was no significant difference in EABR threshold over the course of the stimulation program for any cohort in the present study. There was, however, a small but significant increase in threshold from 184 ± 4 to 199 ± 6 CL over the 28 d period ($p = 0.043$; Two way (Electrode, Time) RM ANOVA) when all stimulated cohorts were combined.

3.3. Cochlear pathology

3.3.1. General cochlear pathology

Electrode insertion trauma was observed in less than 5% of the implanted cochleae in the present study. Because the trauma was localized and very minimal, no cochlea was withdrawn from the study; the tissue response was considered to be predominantly evoked by the presence of the electrode array and/or the chronic stimulation.

3.3.2. Tissue response

Representative examples of the tissue response observed in the scala tympani adjacent to the electrode array are illustrated in figure 3. Implanted control cochleae showed a minimal tissue response (figure 3(a)) while stimulated cochleae evoked a mature fibrous tissue response. This included a thin, dense tissue capsule around the electrode array (electrode tract, ET; figure 3(b)) with mature fibrous tissue

occupying much of the remainder of the scala tympani. A more extensive tissue response was evident at higher charge densities (compare figure 3(b) with figures 3(c)–(h)). This response sometimes included a necrotic zone opposed to the electrode contact (e.g. figure 3(e)) and typically exhibited a zone of macrophages located around a section of the electrode tract (figures 3(c)–(h)). Under some stimulus conditions relatively large amounts of particulate material were evident in the tissue capsule (e.g. figures 3(d), (g)). Minimal fibrous tissue was observed apical to the electrode array and only small amounts of fibrous tissue was present adjacent to the unstimulated region of the electrode array in the LB turn. Finally, although a small number of cochleae exhibited neo-osteogenesis, stimulus-induced new bone formation was not evident in any cochlea.

The cross-sectional area of the tissue response within the UB scala tympani for each cohort is illustrated in figure 4. There was a significant increase in tissue response with charge density ($p = 0.007$, One-way ANOVA); with a post-hoc analysis specifically showing significant increases following stimulation at charge densities ≥ 200 μC cm^{-2} phase^{-1} compared to unstimulated cochleae (p's < 0.012, Holm-Sidak). There was no significant difference in the extent of the tissue response with charge recovery technique (i.e. electrode shorting alone versus electrode shorting with AP or CC; $p = 0.56$, One-way ANOVA).

In addition to an analysis of the total tissue response, histological examination sometimes revealed local sites of necrosis within the tissue capsule consisting of amorphous acellular material bordered by a band of macrophages (figure 2). There was a significant increase in the maximum thickness of the necrosis with charge density ($p = 0.032$, One-way ANOVA; figure 5(a)).

A zone of macrophages were also observed between the electrode tract and the mature fibrous tissue response that occupied the majority of the scala tympani. There was a significant difference in the thickness of the macrophage zone with charge density ($p = 0.025$, One-way ANOVA, figure 5(b)). Finally, there was no significant difference in thickness of the necrotic and macrophage zones with charge recovery technique ($p = 0.54$ & $p = 0.35$ respectively; One-way ANOVA, figures 5(a), (b)).

3.3.3. AN survival
Representative examples of AN survival in the left (i.e. proximal to the electrode array) and right (unimplanted control) cochleae for all cohorts are illustrated in figure 6. The AN density in the control cochleae is typical for guinea pig cochleae following this period of deafening. The close symmetry of AN survival in the implanted unstimulated cochlea and its contralateral control (figure 6(a)), contrasts with an apparent increase in AN survival in a number of

the stimulated cochleae compared with their control cochlea (e.g. figures 6(b), (e), (g)–(i)).

Figure 7 illustrates the mean AN density for all cochlear regions of implanted and contralateral control cochleae. There was no stimulus induced reduction in AN density for any cohort. Indeed, there was a significantly greater AN density in the UB turn of stimulated versus the contralateral control cochlea in cohorts stimulated at 100, 267, 267 CC, 400 and 540 CC μC cm^{-2} phase^{-1} ($p < 0.05$; Paired t-test; figure 7). The remaining cochlear regions showed a symmetrical pattern of neural survival for implanted and control cochleae. Finally, there was no statistically significant difference in AN survival with charge recovery technique ($p = 0.53$; One-way ANOVA).

3.4. Electrode corrosion
SEM imaging of the electrodes was performed in order to evaluate the extent of corrosion across the cohorts. In some cases, the Pt surface was covered with corrosion products and/or tissue that required removal prior to examination of the Pt surface. Micrographs from three electrodes on an array stimulated continuously for 4 weeks at 200 μC cm^{-2} phase^{-1} and 1000 pps (cohort 3) illustrate the typical range of Pt corrosion observed in the present study (figure 8). Electrode E1, an unstimulated control, showed no evidence of corrosion although some manufacturing marks were present (corrosion grade 0; figure 8(a)). Electrode E6, a flanker electrode, was stimulated at ~100 μC cm^{-2} phase^{-1}. This electrode exhibited localised Pt corrosion (grade 2; figure 8(b)). Electrode E7, a centre tripole, was stimulated at 200 μC cm^{-2} phase^{-1}. This electrode surface exhibited widespread pitting corrosion (grade 4; figure 8(c)).

Representative SEM micrographs showing the effectiveness of CC in reducing corrosion on the Pt surface is illustrated in figure 9. The four electrodes were all centre tripole electrodes stimulated at 267 (figures 9(a)–(c)) or 540 μC cm^{-2} phase^{-1} (figure 9(d)) at 200 pps. Figure 9(a) illustrates the extensive corrosion observed following chronic stimulation at 267 μC cm^{-2} phase^{-1} using electrode shorting alone. In contrast, far less corrosion was apparent on the surface of electrodes stimulated at these high charge densities using electrode shorting with CC (figures 9(c), (d)). Finally, the use of AP with electrode shorting reduced the level of corrosion compared with shorting alone, although not to the same extent as CC (figure 9(b)).

The mean corrosion grade for all electrodes in each cohort is illustrated in figure 10. There was no significant difference in electrodes across the array for both the implanted control (cohort 1; $p = 0.84$; $n = 4$) and 100 μC cm^{-2} phase^{-1} cohorts (cohort 2; $p = 0.60$; $n = 5$ ANOVA by Ranks). There was no evidence of corrosion on any electrode among
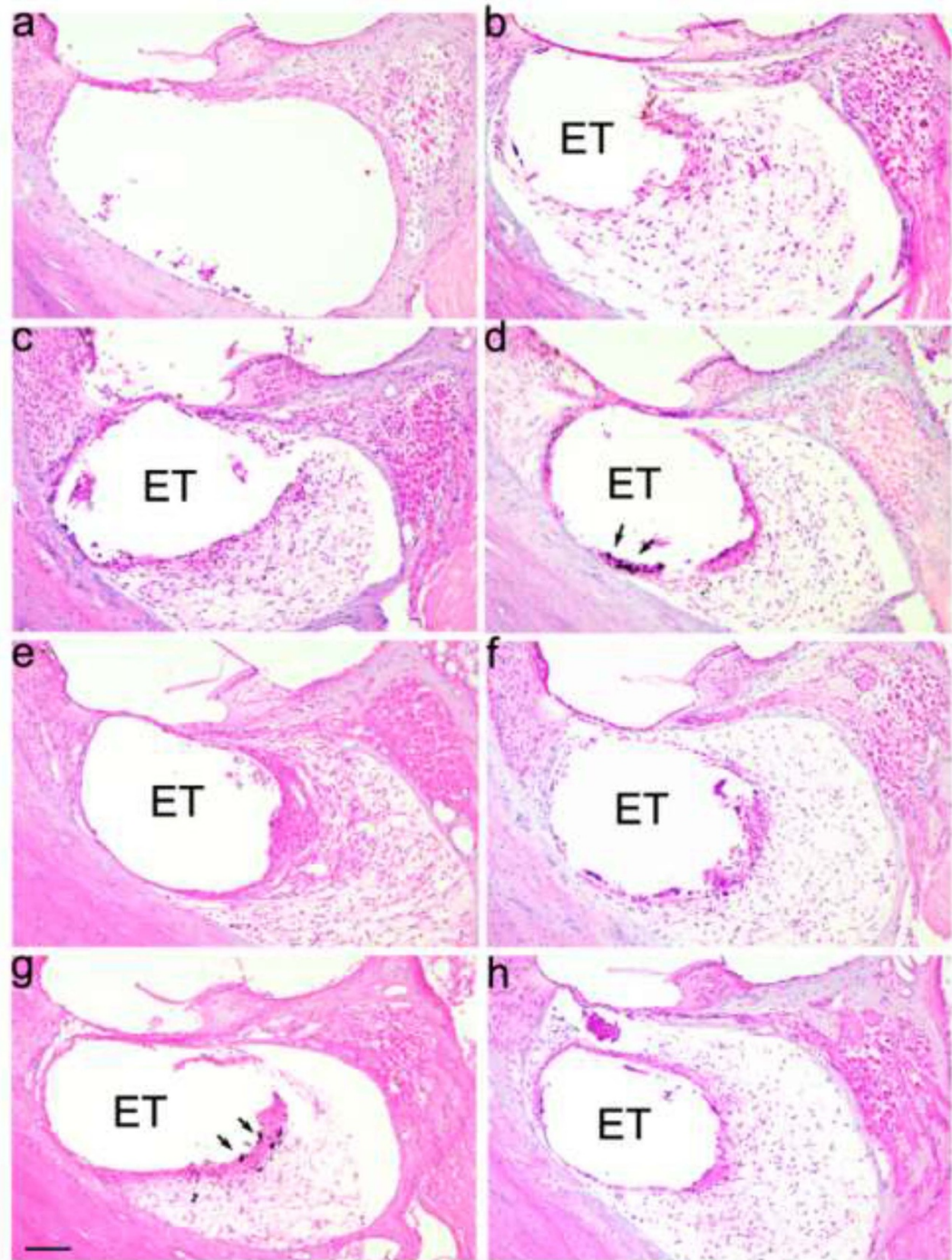
Figure 3. Typical tissue response adjacent to the electrode array in the UB turn. (a) Implanted control cochleae. (b)–(h) All stimulated cochleae showed a clear tissue response. The most widespread response occurred in cochleae stimulated at charge densities ≥ 200 μC cm^{-2} phase^{-1}; (b) 100; (c) 228, (d) 267; (e) 267 AP; (f) 267 CC; (g) 400 and (h) 540 CC μC cm^{-2} phase^{-1}. ET = electrode tract. Arrows illustrate examples of particulate material within the tissue. Scale bar = 100 μm.

these two cohorts (Corrosion grades 0–1). In contrast, there were significant differences in the extent of corrosion across electrodes in all other cohorts and the level of corrosion was dependent on the stimulation history of each electrode. Electrodes E4 and E7 (centre tripoles) in all these cohorts exhibited a significantly greater corrosion grading than unstimulated electrodes ($p < 0.05$; Dunn's post hoc analysis), while both flanker (E3, E5, E6 and E8) and centre tripole electrodes showed significantly greater levels of corrosion compared with the unstimulated electrodes (E1 and E2) in cohorts 3–6 & 8 ($p < 0.05$; Dunn's post hoc analysis). Finally, in the cohorts that exhibited the most extensive corrosion grades (cohorts 5, 6 & 8), the level of corrosion for the centre tripole electrodes were also significantly greater than
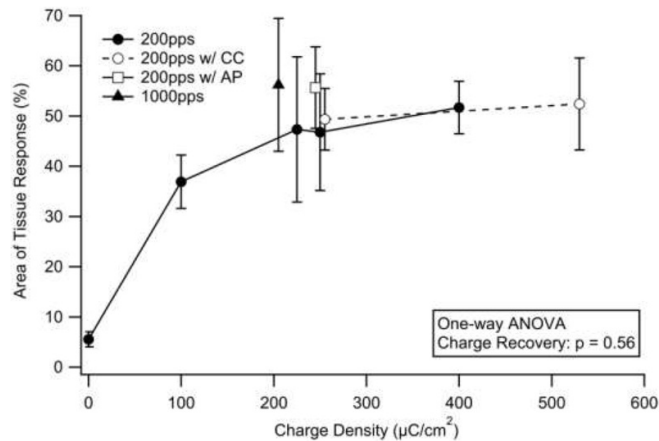
Figure 4. Mean tissue response in the UB turn scala tympani for the nine cohorts in this study. There was a significant difference in the degree of fibrous tissue response with charge density ($p = 0.007$); however, the tissue response was independent of the charge recovery technique ($p = 0.56$). Error bars = sem.
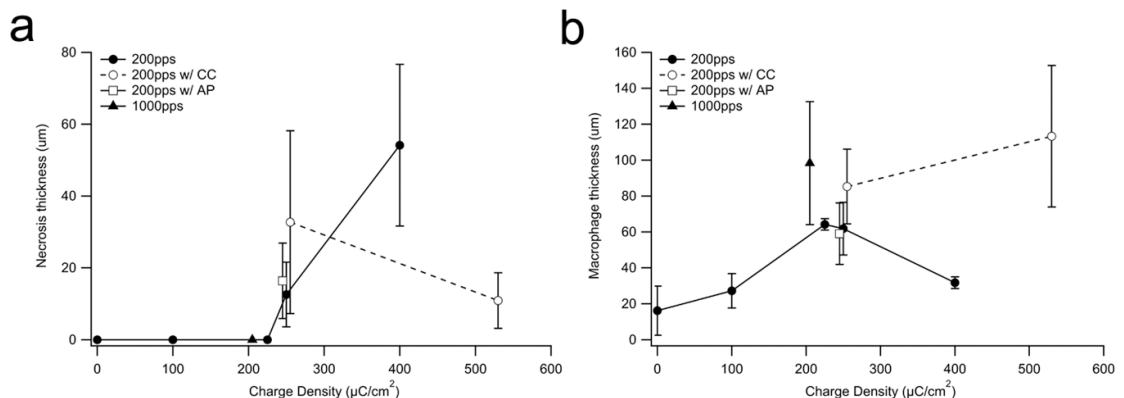

Figure 5. (a) Mean thickness of the necrotic zone versus charge density within the UB turn. Necrosis was only evident in cochleae stimulated at high charge densities ($\geq 267\ \mu C\ cm^{-2}\ phase^{-1}$). The extent of the necrotic zone was not associated with the charge recovery technique ($p = 0.54$). (b) Mean thickness of the macrophage zone within the UB turn. With the exception of cohort 8, thickness of the macrophage zone increased with charge density. This response was independent of the charge recovery technique used ($p = 0.35$). Error bar = sem.

their flanker electrodes ($p < 0.05$; Dunn's post hoc analysis).

3.5. Analysis of particulate deposits

Particulate deposits were evident histologically in all cochleae stimulated at charge densities $\geq 200\ \mu C\ cm^{-2}\ phase^{-1}$ using electrode shorting alone (cohorts 3–5 & 8; e.g. figure 11). These deposits were located in the electrode-tissue capsule of the UB turn proximal to the chronically stimulated tripolar electrodes centred on electrode E7. There was little evidence of particulate material in the tissue capsule of cochleae stimulated at 267 or $540\ \mu C\ cm^{-2}\ phase^{-1}$ that combined electrode shorting with CC (cohorts 7 & 9), and only minor particulate material in one cochlea stimulated at $267\ \mu C\ cm^{-2}\ phase^{-1}$ in the AP cohort (cohort 6).

The majority of the particulate material consisted of sub-micron particles phagocytosed by macrophages, although occasional larger deposits ($< 20\ \mu$m in length) were evident (figure 11). SEM-EDS identified these deposits as Pt (data not illustrated).

Cochleae were examined histologically and qualitatively graded from 0 (no material present) to 4 (widespread particulate material present). Figure 12 illustrates the extent of Pt corrosion products within the scala tympani as a function of charge density. There was a difference in the amount of particulate Pt with both charge density ($p < 0.01$; One way ANOVA) and the charge recovery technique ($p < 0.01$; One way ANOVA, figure 12). Reduced levels of Pt corrosion product were evident in animals stimulated using AP or CC charge recovery techniques.

3.6. Trace analysis of Pt

ICP-MS analysis did not detect Pt in the unimplanted contralateral cochleae at the detection limit of the spectrometer ($0.01\ mg\ kg^{-1}$). In contrast, trace levels
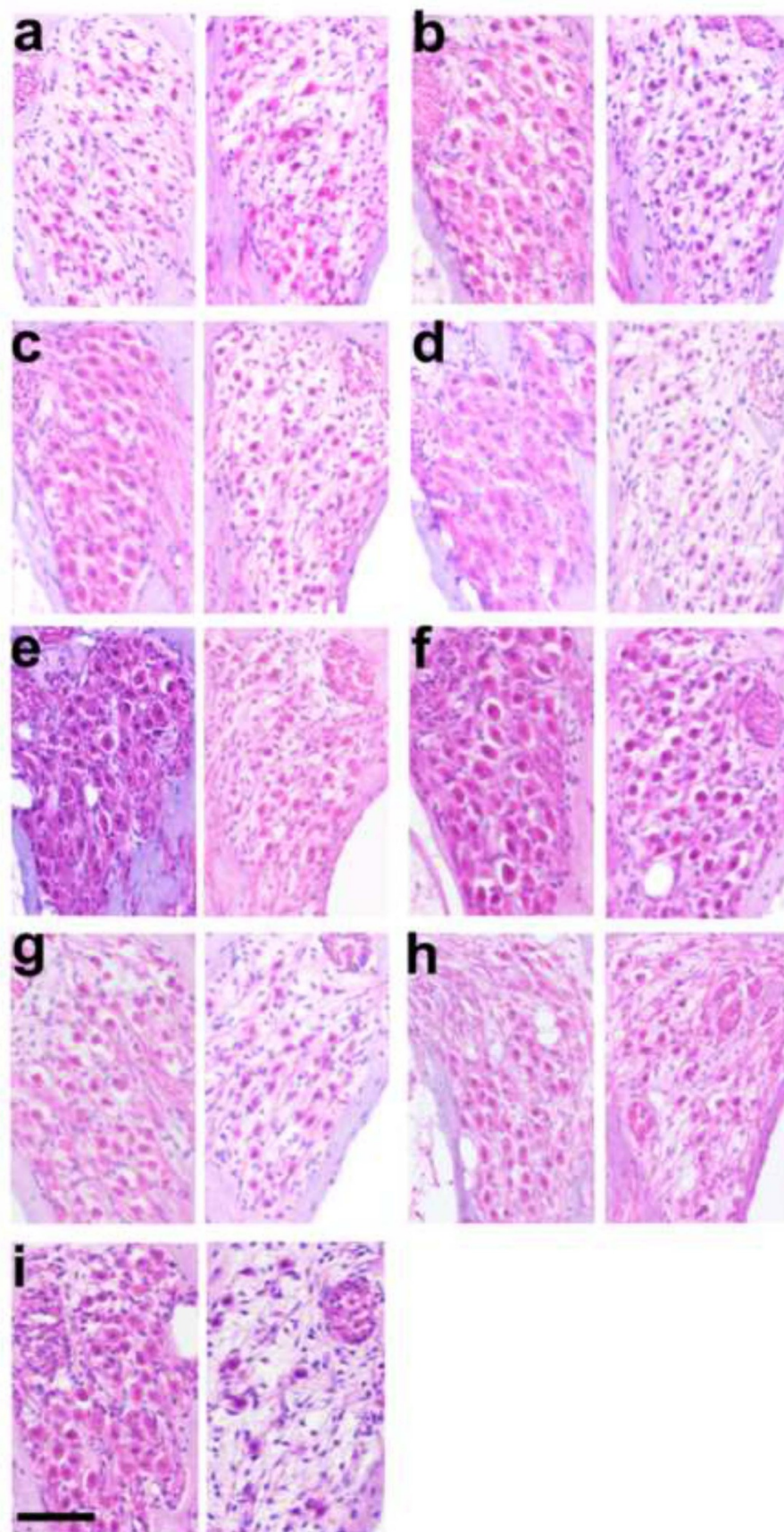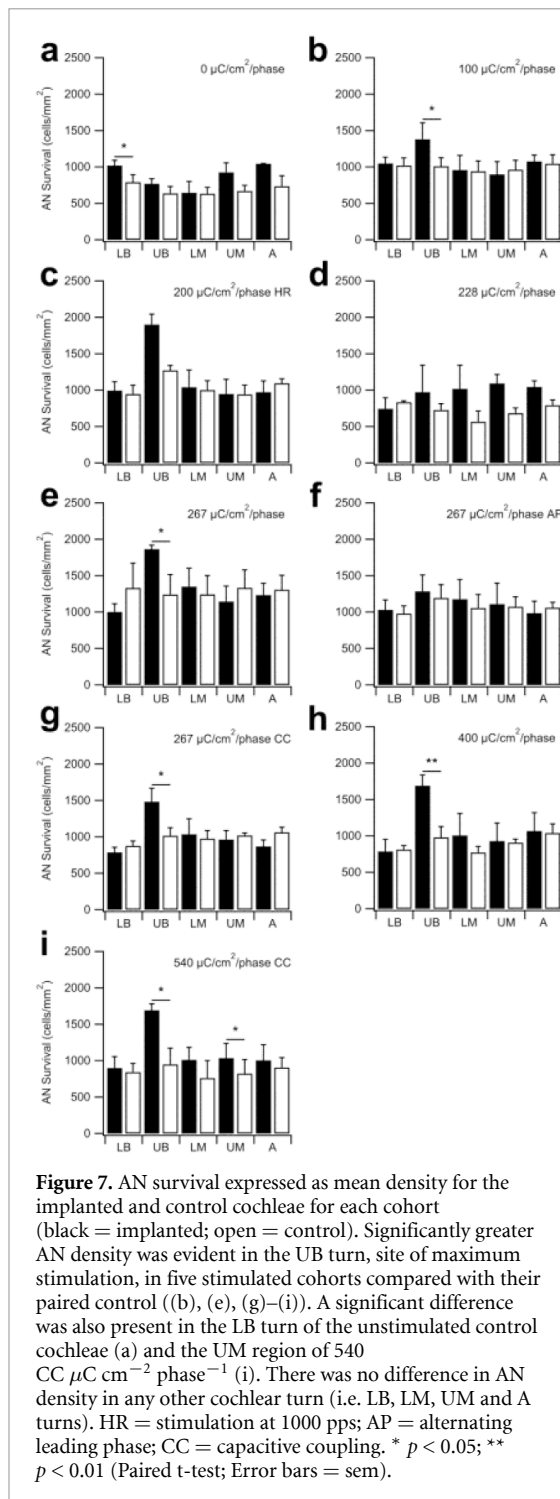
Figure 6. Illustrative micrographs showing AN survival in the UB turn of the left (stimulated) and right (control) cochleae from each of the nine cohorts (table 1). (a) Implanted unstimulated control; (b) 100; (c) 200 at 1000 pps; (d) 228; (e) 267; (f) 267 AP; (g) 267 CC; (h) 400; and (i) 540 μC cm^{-2} phase^{-1} CC. Greater AN survival was observed in some stimulated cohorts when compared to their control cochleae. Scale bar = 50 μm.

Figure 7. AN survival expressed as mean density for the implanted and control cochleae for each cohort (black = implanted; open = control). Significantly greater AN density was evident in the UB turn, site of maximum stimulation, in five stimulated cohorts compared with their paired control ((b), (e), (g)–(i)). A significant difference was also present in the LB turn of the unstimulated control cochlea (a) and the UM region of 540 CC μC cm^{-2} phase^{-1} (i). There was no difference in AN density in any other cochlear turn (i.e. LB, LM, UM and A turns). HR = stimulation at 1000 pps; AP = alternating leading phase; CC = capacitive coupling. * $p < 0.05$; ** $p < 0.01$ (Paired t-test; Error bars = sem).

Table 2. Pt trace analysis data for each stimulated cohort in this study.

Cohort	Stimulation parameters	ng mg^{-1} half cochlea
1	Implanted controls	1
2	100 μC cm^{-2} phase^{-1}; 200 pps	–
3	200 μC cm^{-2} phase^{-1}; 1000 pps	–
4	228 μC cm^{-2} phase^{-1}; 200 pps	124
5	267 μC cm^{-2} phase^{-1}; 200 pps	147
6	267 μC cm^{-2} phase^{-1}; 200 pps; AP	88
7	267 μC cm^{-2} phase^{-1}; 200 pps; CC	61
8	400 μC cm^{-2} phase^{-1}; 200 pps	136
9	540 μC cm^{-2} phase^{-1}; 200 pps; CC	93

Note: – = data not available

observed in cochlear histology; (ii) the extent of Pt corrosion associated with the surface of the electrodes examined under SEM; and (iii) trace analysis of Pt in cochleae measured using ICP-MS. These three techniques showed consistent findings: the level of Pt corrosion increased with charge density and was reduced in cohorts stimulated using electrode shorting with CC or AP. Consistent with our previous report [8], the extent of the tissue reaction in the cochleae was related to charge density; all cochleae stimulated at ≥ 200 μC cm^{-2} phase^{-1} displayed a vigorous tissue reaction that was localized to the stimulation site, and stimulation at high charge densities resulted in a focal region of necrosis and a zone of macrophages close to the Pt electrode. Notably, the extent of the tissue response was not affected by the charge recovery technique, implying that tissue response is not influenced by the amount of particulate Pt within the cochlea. Finally, despite chronic stimulation at intense change densities as high as 540 μC cm^{-2} phase^{-1} producing a vigorous tissue response and Pt corrosion, there was no evidence of stimulus induced adverse effects on ANs or their function.

4.1. Pt dissolution and charge recovery

CC and AP have been shown to eliminate or reduce DC leakage current respectively [13, 14]; it is therefore tempting to speculate that at least part of the process underlying Pt dissolution is associated with DC. However, previous data linking DC and dissolution in neural stimulators is conflicting. Most of the historical work, both *in vivo* and *in vitro*, used CC devices (e.g. [11, 12, 27].). In these cases the DC was zero and yet significant rates of dissolution were reported, suggesting a mechanism unrelated to DC. Moreover, unpublished stimulation experiments in physiological saline by one of the authors (PMC) found little difference between dissolution rates with and without CC. On the other hand, if a constant potential is applied to an electrode in solution, the level of dissolution reduces initially [28] and then stabilises to a level that is a strong function of the level of DC
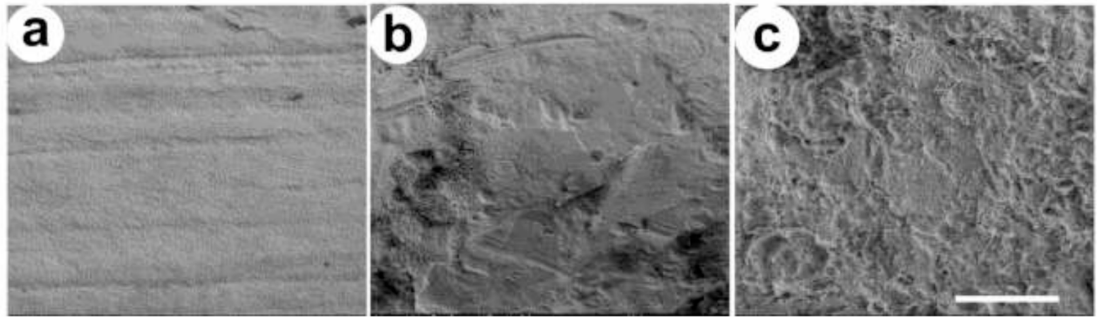
were present in all implanted cochleae including just detectable levels in the implanted, unstimulated control cochleae (cohort 1; table 2). The level of Pt was dependent on the charge density and appeared to be also influenced by the charge recovery technique; reduced levels were associated with CC and, to a lesser extent, with AP.

4. Discussion

We evaluated the amount of Pt corrosion using three measures: (i) the amount of Pt corrosion product

Figure 8. Scanning electron micrographs of the surface of three Pt electrodes from an array chronically stimulated at 200 μC cm^{-2} phase^{-1} and 1000 pps (cohort 3; table 1). (a) Electrode E1 was unstimulated and had a corrosion grade of 0. (b) Electrode E6 was a flanker and had slight Pt corrosion (grade 2). (c) Electrode E7 was a centre tripole electrode and exhibited extensive pitting corrosion across the Pt surface (grade 4). Scale bar = 20 μm.
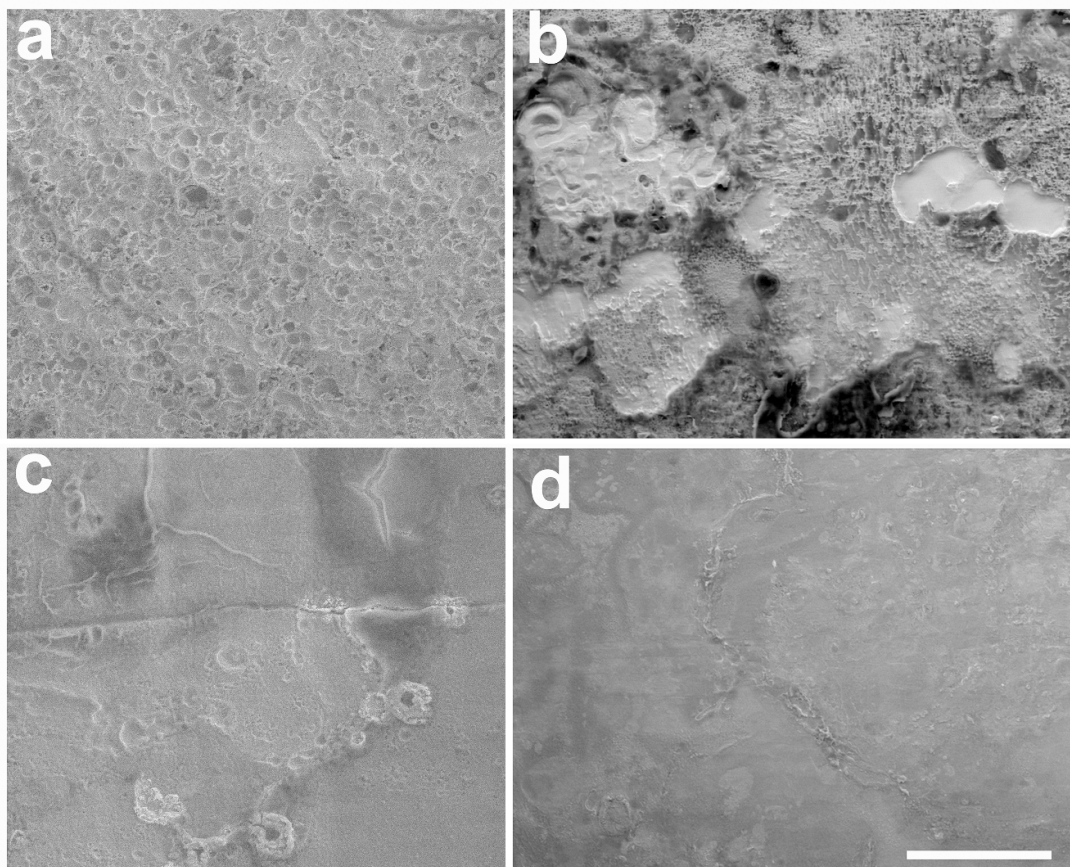

Figure 9. Representative SEM micrographs of 4 centre tripole electrodes showing the effects of charge recovery on Pt corrosion. (a) Corrosion associated with stimulation at 267 μC cm^{-2} phase^{-1} using electrode shorting alone (grade 4). (b) 267 AP μC cm^{-2} phase^{-1} (grade 3). In contrast, stimulation using CC at (c) 267 μC cm^{-2} phase^{-1} (grade 1) or (d) 540 μC cm^{-2} phase^{-1} (grade 1) resulted in far less visible Pt corrosion. All electrodes illustrated were stimulated at 200 pps. Scale bar = 20 μm.

[29]. Clearly DC and dissolution are related in this instance.

Our findings echo the dichotomy observed in the literature. In support of a mechanism unrelated to DC, animals in cohort 3 in the present study were stimulated at significantly higher rates than other cohorts (1000 versus 200 pps). Higher stimulus rates are associated with elevated DC leakage current using electrode shorting [13]; however, there was no marked difference in either the degree of electrode corrosion or particulate Pt within the cochleae of this cohort compared with other groups
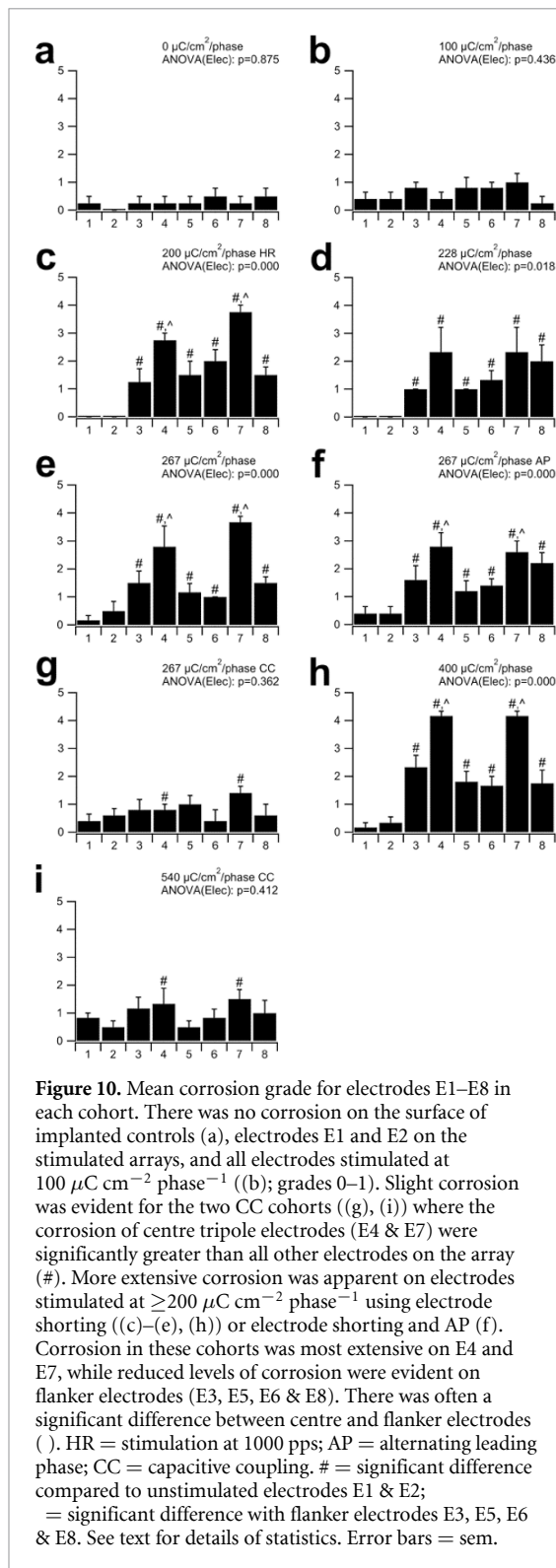
Figure 10. Mean corrosion grade for electrodes E1–E8 in each cohort. There was no corrosion on the surface of implanted controls (a), electrodes E1 and E2 on the stimulated arrays, and all electrodes stimulated at $100 \, \mu C \, cm^{-2} \, phase^{-1}$ ((b); grades 0–1). Slight corrosion was evident for the two CC cohorts ((g), (i)) where the corrosion of centre tripole electrodes (E4 & E7) were significantly greater than all other electrodes on the array (#). More extensive corrosion was apparent on electrodes stimulated at $\geq 200 \, \mu C \, cm^{-2} \, phase^{-1}$ using electrode shorting ((c)–(e), (h)) or electrode shorting and AP (f). Corrosion in these cohorts was most extensive on E4 and E7, while reduced levels of corrosion were evident on flanker electrodes (E3, E5, E6 & E8). There was often a significant difference between centre and flanker electrodes (^). HR = stimulation at 1000 pps; AP = alternating leading phase; CC = capacitive coupling. # = significant difference compared to unstimulated electrodes E1 & E2; ^ = significant difference with flanker electrodes E3, E5, E6 & E8. See text for details of statistics. Error bars = sem.

stimulated at high charge densities. Conversely, the modest reduction in dissolution due to AP (cohort 6) compared to the same phase equivalent (cohort 5), provides an argument for a DC-related mechanism. The effect of AP stimulation is to reduce DC *and* increase the potential range over which the electrode interface transitions. Had the potential range increased (for example, by delivering more charge) without the associated reduction in DC, this would

likely have increased dissolution, suggesting dissolution is dependent on the DC level.

One way to resolve these apparent discrepancies is to propose two mechanisms that contribute to Pt dissolution; one dependent on DC and one not. A good candidate for the DC-independent mechanism is one described by Topalov and colleagues [30], where dissolution occurs due to voltage transitions of the Pt/electrolyte interface through the oxide formation and reduction regions. These transitions occur during the delivery of every stimulus pulse whether or not a coupling capacitor is present. For the DC-dependent findings, the (anodic) oxygen evolution reaction of Pt ($2OH^- => H_2O + \frac{1}{2}O_2 + 2e^-$) is known to promote dissolution [31] and may be the mechanism responsible at anodic potentials. Oxygen evolution is, however, an anodic process and cannot explain the dissolution that occurred at the cathodic-first centre electrodes of our tripoles. A cathodic Pt dissolution mechanism has been described caused by the reduction of molecular oxygen in solution: oxygen is reduced at the cathode to H_2O_2 ($O_2 + 2 H^+ + 2e^- => H_2O_2$) which is then further reduced to the highly oxidising hydroxyl radical OH^0 ($H_2O_2 + e^- => OH^- + OH^0$). Although not fully understood, it is thought this short-live radical may be responsible for Pt dissolution through the oxidation of Pt metal to its ionic form ($2OH^0 + 2Pt => 2Pt^{2+} + 2OH^-$) [32, 33].

The use of CC forces zero DC to flow through an electrode, which in turn forces the total anodic and total cathodic by-products at the electrode to be equal. It does not, as is sometimes thought, eliminate irreversible by-products at the electrode altogether. To achieve this anodic/cathodic balance, CC forces the electrode to change its potential, through the mechanism of slideback [3, 34], to a position that minimises irreversible by-products. This complex set of actions resulting from CC appears to reduce dissolution *in vivo* compared with AP and shorting alone. However, dissolution can still occur at significant levels with CC. For example, CC stimulation at the highest charge density used in the present study ($540 \, \mu C \, cm^{-2} \, phase^{-1}$; cohort 9), resulted in higher levels of Pt in tissue, when considered on a per electrode area basis, than cohort 5 which used half the charge density and electrode shorting. Whether dissolution during CC stimulation predominantly occurs due to the potential transition mechanism [31], an equal combination of irreversible oxidation and reduction reactions (e.g. oxygen evolution during the anodic phase and oxygen reduction during the cathodic phase), or some other mechanism is unclear. Our observations are, however, consistent with other data describing the presence of particulate Pt in all cochlear specimens examined from long-term implant users [7]. These devices used a variety of charge recovery techniques including electrode shorting alone and electrode shorting with CC.
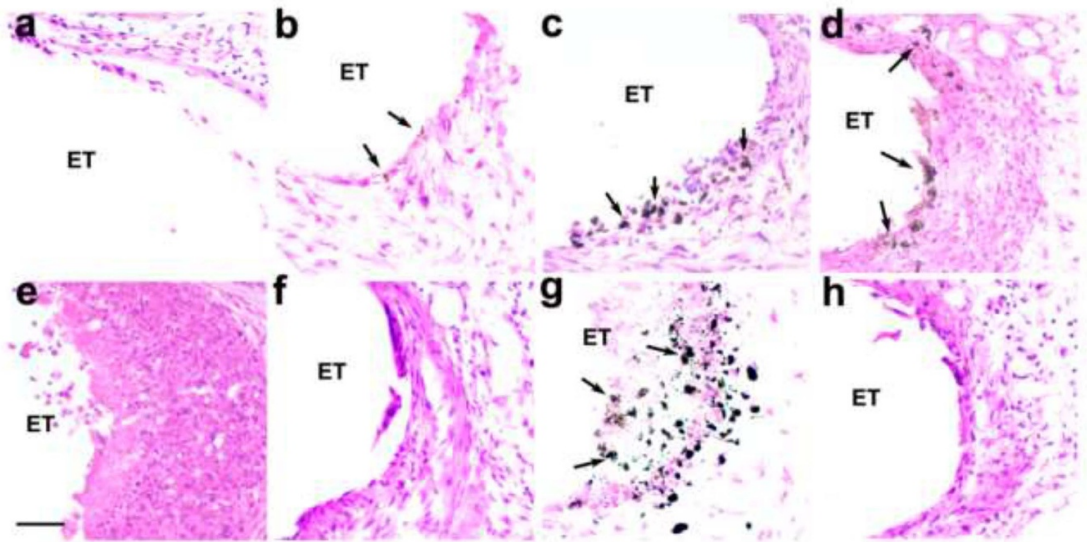
Figure 11. Representative photomicrographs illustrating the electrode-tissue capsule (ET) in the UB turn of eight of the cohorts used in this study. The extent of the particulate deposits (arrows) appeared to vary with both charge density and the technique used to achieve charge balance. (a) Implanted, unstimulated control (cohort 1): (b) 100 μC cm^{-2} phase^{-1} with electrode shorting (cohort 2); (c) 228 μC cm^{-2} phase^{-1} with electrode shorting (cohort 4); (d) 267 μC cm^{-2} phase^{-1} with electrode shorting (cohort 5); (e) 267 μC cm^{-2} phase^{-1} with electrode shorting and AP (cohort 6); (f) 267 μC cm^{-2} phase^{-1} with electrode shorting and CC (cohort 7); (g) 400 μC cm^{-2} phase^{-1} with electrode shorting (cohort 8); (h) 540 μC cm^{-2} phase^{-1} with electrode shorting and CC (cohort 9). ET = electrode tract. Scale bar: 50 μm.
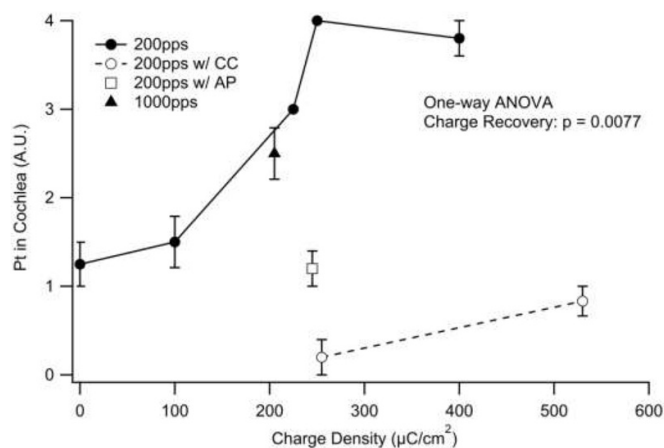

Figure 12. Mean extent of particulate Pt occupying the UB turn scala tympani as a function of charge density. There was a statistically significant increase in Pt corrosion products associated with charge density ($p < 0.01$). The charge recovery technique also appeared to effect corrosion product ($p < 0.01$), with reduced levels associated with AP and CC. Error bars = sem.

The origin of the particulate Pt is unclear. It seems unlikely to result directly from flaking of electrode material as manufactured since all electrode arrays underwent an extensive cleaning program prior to implantation that included sonication, and the unstimulated electrodes surfaces were in general quite smooth (figure 1). In addition, the nature of the particulate Pt observed histologically were sub-micron in size, with the significant majority of particles phagocytosed; Pt fragments produced during manufacture are likely to be considerably larger. Pt and other metals can undergo a surface flaking process known as spalling when electrodes are pulsed repeatedly under certain conditions. The upper and lower potentials reached by the electrode when being pulsed are critical to this process [34]. As noted above, the addition of AP or CC to shorting will modify these potentials and may explain the large difference in particulate scores between shorting alone and shorting with AP or CC, while the trace levels of Pt in tissue show far less variation. Another possibility is that the Pt particles form through reduction of ionic Pt, perhaps due to conditions generated at the cellular level which favour reduction (e.g. $PtCl_4^{2-} + 2e^- => Pt^0 + 4Cl^-$). Such a process may occur when Pt ions are above a certain concentration in tissue.

As we have previously reported [8], the particulate Pt observed histologically was localized to the

tissue capsule close to the electrode tract, and the majority of the Pt was phagocytosed by macrophages although some larger deposits were not. There was little evidence of Pt deposits distal to the electrode-tissue capsule; no Pt was observed in Rosenthal's canal, the scala media, or scala vestibuli.

While the extent of Pt dissolution *in vivo* is related to charge density, the present study does not provide insight into the rate of Pt dissolution over time. A number of previous *in vivo* studies have shown that there is a rapid increase in Pt corrosion product following the onset of stimulation [35], and the rate of this dissolution gradually decreases during stimulation [36], although further research is required to clarify this issue.

The three measures of Pt corrosion used in the present study were complementary and each had a specific methodological strength. Trace analysis using ICP-MS provided a highly sensitive quantitative measure of Pt dissolution, while SEM examination of the electrode surface provided a qualitative measure of corrosion for each electrode on the array that could be related to its specific stimulation history (i.e. centre tripole; flanker or control electrode). Finally, the evaluation of particulate Pt within cochlear histology provided a quantitative estimate of Pt across cohorts as well as insight into the cellular response and the location of the particulate in relation to the electrode-tissue interface.

Although these three methods of evaluating Pt dissolution were in broad agreement, there were some disparities between techniques, presumably as a result of the semi-quantitative assessment method used for the particulate Pt assessment. Specifically, the mean score for particulate Pt observed histologically in implanted unstimulated controls (cohort 1) was ~1 (figure 12) while the corresponding trace analysis for Pt was 1 ng mg^{-1} half^{-1} cochlea (table 2). In contrast, particulate Pt scores for cochleae stimulated using CC and shorting (cohorts 7 and 9) were between 0 and 1 (figure 12). While these results could be interpreted as evidence that CC has a preventative effect on Pt corrosion, corresponding trace analysis of Pt within the cochleae show this is not the case, with corresponding trace Pt levels of 61 and 93 ng mg^{-1} half^{-1} cochleae (table 2). We attribute this discrepancy to the grading method associated with the particulate Pt scoring, in particular the potential for lack of precision when assessing levels 0 (no particulate material in any section) and 1 (possible particulate material present).

Finally, there were trace levels of Pt in the implanted, unstimulated control cochleae (cohort 1), albeit two orders of magnitude less than that observed in stimulated cochleae. While it is possible that this level of Pt may be associated with small fragments of the metal flaking off the electrode surface, we cannot dismiss the possibility that Pt electrodes undergo small amounts of corrosion *in vivo* in the absence of stimulation as has been previously reported for unstimulated microelectrodes [37]. Longer-term studies evaluating Pt corrosion in implanted control cochleae are warranted.

4.2. Tissue response and Pt dissolution

The tissue response in the present study was in the form of a mature foreign body response that included a compact tissue capsule around the array, and loose, well vascularized fibrous tissue within the remainder of the scala tympani proximal to the electrode array. These findings are consistent with previous studies examining the inflammatory response associated with cochlear implantation [38, 39]. In addition to this mature tissue response, cochleae stimulated at levels ≥267 μC cm^{-2} phase^{-1} displayed local necrosis associated with the tissue capsule consisting of amorphous acellular material typically surrounded by a band of macrophages. The position and dimensions of this focal necrosis was consistent with the dimensions of the Pt electrode, and is likely to be associated with the presence of local toxic by-products associated with these high charge densities.

The present findings support our previous observations showing a clear relationship between electrical stimulation at moderate to high charge densities and a vigorous tissue response restricted to the region proximal to the electrode array [8]. In cochlear regions apical to the array there was a minimal tissue response. These results are also consistent with clinical findings reporting that the formation of a vigorous tissue capsule around the electrode array [40].

As noted above, we described local regions of necrosis near the stimulating electrodes. A similar response was reported by Agnew and colleagues following intracortical stimulation [35]. Although all implanted cochleae examined in the present study contained trace levels of Pt, our results indicate that the necrotic response was unrelated to the presence of Pt corrosion product observed histologically.

4.3. Relationship to the defined safety limits for Pt electrodes

Cochlear implants follow the Association for the Advancement of Medical Instrumentation (AAMI) standard for commercial cochlear implants [22]. This standard is based on a Shannon limit of $k = 1.75$ and a maximum charge density of 216 μC cm^{-2} phase^{-1} as the safe limit [22]. The present study included stimulus parameters well above this standard, achieving $k = 2.0$ for the highest charge density (540 μC cm^{-2} phase^{-1}); a 77% greater charge density and more than 300% more than Shannon's proposed limit of $k = 1.5$ [41].

While these stimulus levels did not damage ANs or the cochlea in general, the detection of trace levels of Pt and evidence of Pt corrosion associated with electrodes stimulated at levels less than

216 μC cm^{-2} phase^{-1}, suggest that Pt dissolution would occur within this limit. It should be noted, however, that typical clinical levels of cochlear implant stimulation are approximately an order of magnitude lower than the recommended AAMI limit.

4.4. Status of ANs

There was no stimulus-induced reduction in AN survival in any cohort in the present study, despite stimulation at high charge densities and the presence of significant levels of Pt corrosion. Indeed, in contrast to contralateral control cochleae, we reported a statistically greater AN survival close to the site of stimulation in a number of cohorts stimulated at very high charge densities. Although not consistently observed across cohorts, the results indicate the possibility of a stimulus-induced rescue effect of ANs in response to the normal pattern of degeneration that occurs following deafness [42]. Similar effects have been reported previously [43].

The functional status of ANs was monitored by measuring the change in EABR threshold recorded prior and on completion of the stimulation program. There was no significant increase in EABR threshold for any stimulated cohort in the present study. These data support the conclusion that stimulation across the charge densities used in the present study did not adversely affect ANs.

4.5. Electrode impedance, electrode surface area, and Pt corrosion

There was a small but significant overall increase in impedance over the 28 d stimulation period. While pitting corrosion, observed on centre tripole electrodes stimulated at $\geq$200 μC cm^{-2} phase^{-1}, would produce an increase in the real surface area of the electrode, it is likely that any resultant reduction in impedance would be reversed by a more extensive fibrous tissue response. Given these competing factors—a simultaneous increase in both real surface area and tissue response—more detailed impedance monitoring, such as electrochemical impedance spectroscopy, may provide greater insight into the electrical properties of both the electrode and the tissue interface [9, 44].

The present study used charge densities over an order of magnitude larger than clinical levels in order to provoke and accelerate Pt dissolution mechanisms. Despite the extent of Pt dissolution reported here, accumulated Pt corrosion products do not appear to be associated with any untoward effects on the cochlea. The extent of Pt dissolution would not apply to devices in clinical use because of the large difference in charge densities. However, the development of smaller electrode contacts using thin Pt films reduces the likely dissolution life of an electrode. *In vivo* studies examining the dissolution rates of thin film Pt electrodes considered for clinical application should be undertaken in order to compare with that of bulk Pt electrodes [45].

Finally, it is important to note that charge density in the present study was varied by varying the surface area of the electrodes across cohorts. *In vitro* studies have shown that smaller surface area Pt electrodes have a proportionally higher charge-carrying capacity resulting in an increase in the charge injection limits of the electrode and more efficient tissue activation [46]. Although it is not clear how these effects influence Pt dissolution and tissue response reported in the present study, it is important to note the differences in electrode performance with electrode surface area.

4.6. Clinical implications

Histological studies of cochleae from patients that were long-term cochlear implant users describe particulate Pt within the tissue capsule surrounding the electrode array [4–7]. In one study, particulate Pt was observed in all 45 cochleae examined; the study included a variety of commercial devices [7], indicating that Pt corrosion product is relatively common in cochleae of long-term cochlear implant users. Despite the important clinical implications, little is known about the long-term effects of Pt within the body, although the present study and our previous research [8] suggests that there are no untoward effects associated with Pt within the cochlea.

Clinically, the major source of systemic Pt is associated with the use of Pt-based chemotherapy drugs such as Cisplatin [47, 48]. Typically administered intravenously, Pt accumulates in the kidney, liver and spleen [48]. At high doses Cisplatin is nephrotoxic, although this is thought to be associated with the cellular mechanisms associated with its effect on tumours rather that the toxicity of Pt *per se* [47].

Longer-term *in vivo* studies are required to corroborate the present findings that stimulus-induced Pt corrosion does not adversely affect ANs or the cochlea in general. Moreover, although all Pt deposits in the present study were localized to the electrode-tissue interface, there are no data on the potential for Pt accumulation in other organs. This work is currently under investigation in our laboratory.

Finally, although the post-mortem evaluation of tissue from patients implanted with other neural prostheses appears not to be as extensive as cochlear implant recipients, it is possible that Pt corrosion products will be present in these tissues. For example, a recent report describes evidence of degradation of Pt electrodes following long-term implantation of a cortical visual prosthesis [49], while there are reports of electron dense particulate material obtained from tissue samples of DBS patients [50, 51]. One study described multinucleated giant cells and macrophages with highly electron-dense

inclusions thought to represent phagocytosed material at the electrode-tissue interface [51]. While the authors did not identify the nature and origin of the material, it is likely to be Pt corrosion product. Examination of post-mortem tissue from long-term neural prosthesis users to evaluate the presence and extent of Pt corrosion products and tissue response is recommended.

5. Conclusions

Long-term intracochlear stimulation at intense charge densities of up to 540 μC cm^{-2} phase^{-1} showed that Pt corrosion product was dependent on charge density. The level of corrosion reduced with the use of charge recovery techniques including electrode shorting with CC and, to a lesser extent, electrode shorting with AP. It would appear it is not possible to completely eliminate Pt accumulation as trace levels were also detected in implanted, unstimulated cochleae. The tissue response, which included localized necrotic and macrophage sites proximal to the electrode contact, and a mature fibrous tissue response within the scala tympani, were also charge density dependent. However, the amount of Pt corrosion product did not influence the tissue response. Finally, the presence of Pt corrosion product and/or chronic stimulation at high charge densities did not adversely affect the ANs.

ORCID iDs

Robert K Shepherd ● https://orcid.org/0000-0002-4239-3362
Paul M Carter ● https://orcid.org/0000-0001-9286-1630
Ya Lang Enke ● https://orcid.org/0000-0002-0124-7481
Alex Thompson ● https://orcid.org/0000-0002-8012-872X
Ella P Trang ● https://orcid.org/0000-0003-2009-6671
Ashley N Dalrymple ● https://orcid.org/0000-0001-8566-7178
James B Fallon ● https://orcid.org/0000-0003-2686-3886

References

[1] Shepherd R K, Villalobos J, Burns O and Nayagam D A X 2018 The development of neural stimulators: a review of preclinical safety and efficacy studies *J. Neural. Eng.* **15** 041004

[2] Cogan S F, Ludwig K A, Welle C G and Takmakov P 2016 Tissue damage thresholds during therapeutic electrical stimulation *J. Neural. Eng.* **13** 021001

[3] Merrill D R, Bikson M and Jefferys J G 2005 Electrical stimulation of excitable tissue: design of efficacious and safe protocols *J. Neurosci. Methods* **141** 171–98

[4] Clark G M *et al* 2014 Biomedical studies on temporal bones of the first multi-channel cochlear implant patient at the university of Melbourne *Cochlear Implants Int.* **15** S1-S15

[5] Spiers K, Cardamone T, Furness J B, Clark J C M, Patrick J F and Clark G M 2016 An X-ray fluorescence microscopic analysis of the tissue surrounding the multi-channel cochlear implant electrode array *Cochlear Implants Int.* **17** 129–31

[6] Nadol J B Jr., O'Malley J T, Burgess B J and Galler D 2014 Cellular immunologic responses to cochlear implantation in the human *Hear. Res.* **318** 11–17

[7] O'Malley J T, Burgess B J, Galler D and Nadol J B Jr. 2017 Foreign body response to silicone in cochlear implant electrodes in the human *Otol. Neurotol.* **38** 970–7

[8] Shepherd R K, Carter P, Enke Y L, Wise A K and Fallon J B 2019 Chronic intracochlear electrical stimulation at high charge densities results in platinum dissolution but not neural loss or functional changes in vivo *J. Neural. Eng.* **16** 026009

[9] Cogan S F 2008 Neural stimulation and recording electrodes *Annu. Rev. Biomed. Eng.* **10** 275–309

[10] Shepherd R K, Fallon J B and McDermott H 2014 Medical Bionics *Comprehensive Biomedical Physics* vol 10, ed A Brahme (Amsterdam: Elsevier) pp 327–41

[11] Brummer S B and Turner M J 1977 Electrochemical considerations for safe electrical stimulation of the nervous system with platinum electrodes *IEEE Trans. Biomed. Eng.* **24** 59–63

[12] Robblee L S and Rose T L 1990 Electrochemical guidelines for selection of protocols and electrode materials for neural stimulation *Neural Prostheses—Fundamental Studies*, ed W F Agnew and D B McCreery (Englewood Cliffs, NJ: Prentice Hall) pp 25–66

[13] Huang C Q, Shepherd R K, Carter P M, Seligman P M and Tabor B 1999 Electrical stimulation of the auditory nerve: direct current measurement in vivo *IEEE Trans. Biomed. Eng.* **46** 461–70

[14] Huang C Q, Carter P M and Shepherd R K 2001 Stimulus induced pH changes in cochlear implants: an in vitro and in vivo study *Ann. Biomed. Eng.* **29** 791–802

[15] Swiontek T, Maiman D, Sances A Jr. , Myklebust J, Larson S and Hemmy D 1980 Effect of electrical current on temperature and pH in cerebellum and spinal cord *Surg. Neurol.* **14** 365–9

[16] Shepherd R K, Linahan N, Xu J, Clark G M and Araki S 1999 Chronic electrical stimulation of the auditory nerve using non-charge- balanced stimuli *Acta Otolaryngol.* **119** 674–84

[17] Patrick J F, SeIigman P M, Money D K and Kuzma J A 1990 Engineering *Cochlear Prostheses*, ed G M Clark, Y C Tong and J F Patrick (Edinburgh: Churchill Livingston) pp 99–124

[18] Landry T G, Fallon J B, Wise A K and Shepherd R K 2013 Chronic neurotrophin delivery promotes ectopic neurite growth from the spiral ganglion of deafened cochleae without compromising the spatial selectivity of cochlear implants *J. Comp. Neurol.* **521** 2818–32

[19] Xu J, Shepherd R K, Millard R E and Clark G M 1997 Chronic electrical stimulation of the auditory nerve at high stimulus rates: a physiological and histopathological study *Hear. Res.* **105** 1–29

[20] Shepherd R K, Coco A, Epp S B and Crook J M 2005 Chronic depolarization enhances the trophic effects of brain-derived neurotrophic factor in rescuing auditory neurons following a sensorineural hearing loss *J. Comp. Neurol.* **486** 145–58

[21] Senn P 2015 Neurostimulation for the management of pain *PhD Thesis* University of Melbourne, Melbourne

[22] ANSI 2017 Cochlear implant systems: requirements for safety, functional verification, labeling and reliability reporting *ANSI/AAMI CI86: 2017* AAMI, Arlington, VA p 169

[23] Wise A K, Tan J, Wang Y, Caruso F and Shepherd R K 2016 Improved auditory nerve survival with nanoengineered supraparticles for neurotrophin delivery into the deafened cochlea *PloS One* **11** e0164867

[24] Leake-Jones P A and Rebscher S J 1983 Cochlear pathology with chronically implanted scala tympani electrodes *Ann. New York Acad. Sci.* **405** 203–23

[25] Shepherd R K, Wise A K, Enke Y L, Carter P M and Fallon J B 2017 Evaluation of focused multipolar stimulation for cochlear implants: a preclinical safety study *J. Neural. Eng.* **14** 046020

[26] Dalrymple A N *et al* 2019 Electrochemical and mechanical performance of reduced graphene oxide, conductive hydrogel, and electrodeposited Pt-Ir coated electrodes: an active in vitro study *J. Neural. Eng.* **17** 016015

[27] McHardy J, Robblee L S, Marston J M and Brummer S B 1980 Electrical stimulation with pt electrodes. IV. Factors influencing Pt dissolution in inorganic saline *Biomaterials* **1** 129–34

[28] Topalov A A, Katsounaros I, Auinger M, Cherevko S, Meier J C, Klemm S O and Mayrhofer K J 2012 Dissolution of platinum: limits for the deployment of electrochemical energy conversion *Angew. Chem., Int. Ed.* **51** 12613–5

[29] Black R C and Hannaker P 1980 Dissolution of smooth platinum electrodes in biological fluids *Appl. Neurophysiol.* **42** 366–74

[30] Topalov A A, Cherevko S, Zeradjanin A R, Meier J C, Katsounaros I and Mayrhofer K J J 2014 Towards a comprehensive understanding of platinum dissolution in acidic media *Chem. Soc.* **5** 631–8

[31] Cherevko S, Zeradjanin A R, Topalov A A, Kulyk N, Katsounaros I and Mayrhofer K J J 2014 Dissolution of noble metals during oxygen evolution in acidic media *Chem. Cat. Chem.* **6** 2219–23

[32] Percival S J, Dick J E and Bard A J 2017 Cathodically dissolved platinum resulting from the O_2 and H_2O_2 reduction reactions on platinum ultramicroelectrodes *Anal. Chem.* **89** 3087–92

[33] Noel J-M, Yu Y and Mirkin M V 2013 Dissolution of Pt at moderately negative potentials during oxygen reduction in water and organic media *Langmuir* **29** 1346–50

[34] Donaldson N N and Donaldson P E 1986 Performance of platinum stimulating electrodes mapped on the limit-voltage

plane. Part 2. Corrosion in vitro *Med. Biol. Eng. Comput.* **24** 431–8

[35] Agnew W F, Yuen T G, McCreery D B and Bullara L A 1986 Histopathologic evaluation of prolonged intracortical electrical stimulation *Exp. Neurol.* **92** 162–85

[36] Robblee L S, McHardy J, Agnew W F and Bullara L A 1983 Electrical stimulation with Pt electrodes. VII. Dissolution of Pt electrodes during electrical stimulation of the cat cerebral cortex *J. Neurosci. Methods* **9** 301–8

[37] Barrese J C, Aceros J and Donoghue J P 2016 Scanning electron microscopy of chronically implanted intracortical microelectrode arrays in non-human primates *J. Neural. Eng.* **13** 026003

[38] Foggia M J, Quevedo R V and Hansen M R 2019 Intracochlear fibrosis and the foreign body response to cochlear implant biomaterials *Laryngoscope Investig. Otolaryngol.* **4** 678–83

[39] Bas E *et al* 2015 Spiral ganglion cells and macrophages initiate neuro-inflammation and scarring following cochlear implantation *Front. Cell. Neurosci.* **9** 303

[40] Ishai R, Herrmann B S, Nadol J B Jr. and Quesnel A M 2017 The pattern and degree of capsular fibrous sheaths surrounding cochlear electrode arrays *Hear. Res.* **348** 44–53

[41] Shannon R V 1992 A model of safe levels for electrical stimulation *IEEE Trans. Biomed. Eng.* **39** 424–6

[42] Wise A K, Pujol R, Landry T G, Fallon J B and Shepherd R K 2017 Structural and ultrastructural changes to type I spiral ganglion neurons and Schwann cells in the deafened guinea pig cochlea *J. Assoc. Res. Otolaryngol.* **18** 751-69

[43] Leake P A, Snyder R L, Hradek G T and Rebscher S J 1995 Consequences of chronic extracochlear electrical stimulation in neonatally deafened cats *Hear. Res.* **82** 65–80

[44] Dalrymple A N, Robles U A, Huynh M, Nayagam B A, Green R A, Poole-Warren L A, Fallon J B and Shepherd R K 2020 Electrochemical and biological performance of chronically stimulated conductive hydrogel electrodes *J. Neural. Eng.* **17** 026018

[45] Dalrymple A N, Huynh M, Nayagam B A, Lee C, Weiland G R, Petrossians A, J J, Iii W, Fallon J B and Shepherd R K 2020 Electrochemical and biological characterization of thin-film platinum-iridium alloy electrode coatings: a chronic in vivo study *J. Neural. Eng.* **17** 036012

[46] Green R A, Toor H, Dodds C and Lovell N H 2012 Variation in performance of platinum electrodes with size and surface roughness *Sensors Mater.* **24** 165–80

[47] Miller R P, Tadagavadi R K, Ramesh G and Reeves W B 2010 Mechanisms of cisplatin nephrotoxicity *Toxins* **2** 2490–518

[48] Madias N E and Harrington J T 1978 Platinum nephrotoxicity *Am. J. Med.* **65** 307–14

[49] Towle V L, Pytel P, Lane F, Plass J, Frim D M and Troyk P R 2020 Postmortem investigation of a human cortical visual prosthesis that was implanted for 36 years *J. Neural. Eng.* **17** 045010

[50] Haberler C, Alesch F, Mazal P R, Pilz P, Jellinger K, Pinter M M, Hainfellner J A and Budka H 2000 No tissue damage by chronic deep brain stimulation in Parkinson's disease *Ann. Neurol.* **48** 372–6

[51] Moss J, Ryder T, Aziz T Z, Graeber M B and Bain P G 2004 Electron microscopy of tissue adherent to explanted electrodes in dystonia and Parkinson's disease *Brain* **127** 2755–63